Photoinduced Electron Transfer between the Interlocked Components of Porphyrin Catenanes: Effect of the Presence of Nonequivalent Reduction Sites on the Charge Recombination Rate

Lucia Flamigni,*[a] Anna Maria Talarico,[a] Scolastica Serroni,*[b] Fausto Puntoriero,[b] Maxwell J. Gunter,[c] Martin R. Johnston,[c][+] and Tyrone P. Jeynes[c]

Abstract: [2]Catenanes made up of several polyether-strapped porphyrin macrocycles interlinked with the cyclic electron acceptor cyclo*bis*(paraquat-*p*-phenylene) were spectroscopically, photophysically, and electrochemically characterized. The catenanes exhibit very rich redox behavior due to the presence of several different and interacting electro-active subunits. The redox patterns represent useful "fingerprints" that provide detailed information on the electronic interactions and the chemical environments that the electroactive subunits experience in the supramolecular arrays. A photoinduced electron transfer from the porphyrin excited state (charge separation CS) occurs with $\tau =$ 20 ps in the catenanes with a larger strap and faster than 20 ps (instrumental resolution) in the catenanes with a shorter strap. The resulting charge-separated state recombines to the ground state (charge recombination CR) with lifetimes similar in all cases, 41 ± 4 ps. Comparison of the electron transfer rates CS and CR in the host–guest complexes of the same porphyrins with the noncyclic electron acceptor paraquat, indicate slower reactions in the [2]catenanes. This behavior is assigned to the different separation between reacting partners determined by the type of bond (weak interaction or mechanical) and to a two-step consecutive electron transfer to different sites of the macrocyclic electron acceptor in the catenanes which retards charge recombination.

Keywords: catenanes · electrochemistry · electron transfer · photochemistry · porphyrinoids

Introduction

Porphyrins are photo- and electroactive components with outstanding properties which have been widely used since the early stages of supramolecular photochemistry in the construction of multipartite systems able to respond to light input.[1] Their use was at first essentially based on a biomimetic approach to achieve light energy conversion. From the earliest stages of research into natural photosynthetic phenomena, it was recognized that highly specialized functions such as energy collection and charge separation are performed by organized structures essentially based on porphyrins or closely related chromophores.[2, 3]

In the following decades the use of porphyrins and related components rapidly developed into several fields, and their utilization in the construction of complex architectures for molecular recognition,[4] and in the development of novel materials is of particular note.[5] Their ease of preparation has contributed to a ready availability. The robustness, especially in relation to the possibility of finely tuning their spectroscopic and electrochemical properties by simple substitution or metalation,[6] makes porphyrins very convenient building blocks in the construction of systems able to perform light-triggered functions. Moreover this class of molecules, due to the intense spectroscopic signatures associated with radicals and/or excited states, is particularly well-suited for time-resolved spectroscopic investigations and their study has greatly contributed to the fundamental knowledge of photoinduced energy and electron transfer processes.[7–9]

Porphyrinic units have often been included in potential host or guest systems able to self-assemble in higher order architectures,[7] as well as in multicomponent covalently

[a] Dr. L. Flamigni, Dr. A. M. Talarico
Istituto ISOF-CNR
Via P. Gobetti 101, 40129 Bologna (Italy)
E-mail: flamigni@frae.bo.cnr.it

[b] Dr. S. Serroni, Dr. F. Puntoriero
Dipartimento di Chimica Inorganica
Chimica Analitica e Chimica Fisica, Università di Messina
98166 Messina (Italy)
E-mail: serroni@chem.unime.it

[c] Prof. M. J. Gunter, Dr. M. R. Johnston,[+] Dr. T. P. Jeynes
Department of Chemistry
University of New England, Armidale, NSW 2351 (Australia)

[+] Present address: School of Chemistry, Physics and Earth Sciences,
Flinders University, Bedford Park,
Adelaide, SA 5042 (Australia)

 DOI: 10.1002/chem.200204502

linked systems[8] or in interlocked systems.[9] In this case the aim is to trigger, upon light absorption, some useful and predetermined function such as energy or electron transfer, or some specific molecular motion.

We have recently reported on the photoinduced electron transfer between Zn^{II} porphyrin electron donors and the paraquat electron acceptor within complexes formed by paraquat with a series of porphyrins strapped with polyether chains of different length and with different structures and substitution patterns.[10] The effect of strap length, type, and substitution on the electron transfer rate has been discussed and evidence of complete recombination of the charge-separated state within all complexes has been provided.[10] Herein we describe the spectroscopic, photophysical, and electrochemical characterization of a series of [2]catenanes,[11] in which some of the strapped porphyrins previously studied are now interlocked to the electron acceptor cyclobis(paraquat-*p*-phenylene) ($CBPQ^{4+}$) to yield the catenanes designated Cat-*n* (Figure 1). The cyclic paraquat derivative $CBPQ^{4+}$ has been often used as electron acceptor in interlocked structures by several groups and its properties are well assessed.[12–13] We intend to compare the electron transfer rates in the mechanically linked [2]catenanes Cat-*n*, with the corresponding host–guest complexes previously studied and reported in Figure 1, *n*-PQ^{2+}, with the aim of deriving information on the effect of the linkage (mechanical versus noncovalent) and of the acceptor type on the electron transfer rates in the two different systems.

Results and Discussion

The models

Spectroscopic and photophysical determinations: The photophysical properties of unstrapped porphyrin MOD, of strapped porphyrins, *n*, and of their complexes with PQ^{2+}, *n*-PQ^{2+}, have been previously studied in the context of a detailed photophysical study of a representative series of strapped porphyrins and of their complexes.[10]

The association constants of the complexes in acetonitrile were derived both by spectrophotometric and spectrofluorimetric titrations and are $3 \times 10^4\,M^{-1}$ for **4**-PQ^{2+}, $4 \times 10^2\,M^{-1}$ for **5**-PQ^{2+}, and $4 \times 10^3\,M^{-1}$ for **6**-PQ^{2+}. The properties of the complexes were determined in solutions containing $>95\,\%$ of the porphyrin in the complexed form. Table 1 summarizes the absorption parameters of the porphyrin components and the complexes, while Table 2 collects the luminescence properties of the model porphyrins.

Electrochemical determination: Problems arising from the low solubility of the strapped porphyrins in acetonitrile prevented any electrochemical study in this solvent. The porphyrins were dissolved to the desired concentration ($>5 \times 10^{-4}\,M$) in dimethylformamide (DMF) which permits only a rather modest window to be examined (oxidation wave <0.8 V versus SCE). This allowed only the first oxidation wave of the porphyrins to be determined at $+0.62$, $+0.65$, and

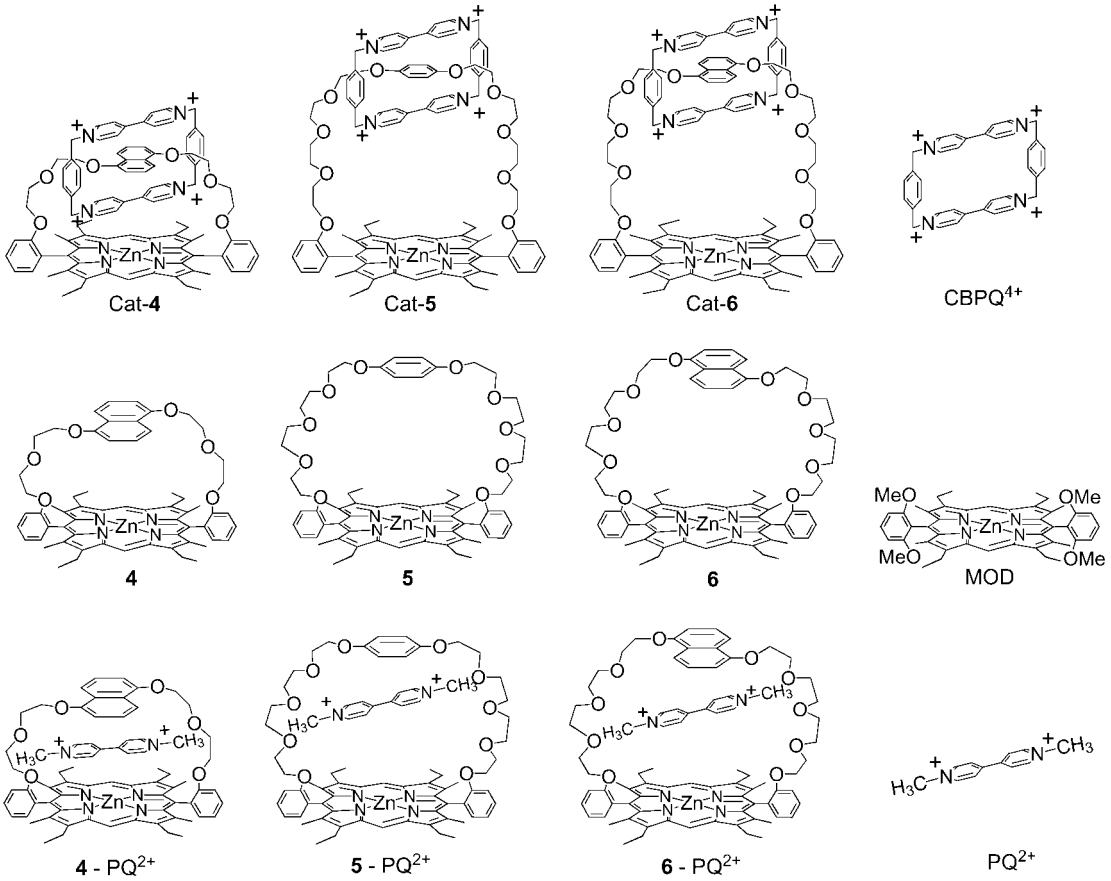

Figure 1. Schematic formulae of the strapped porphyrins *n*, the model MOD, the guests PQ^{2+} and $CBPQ^{4+}$, the complexes and the catenanes

Table 1. Ground state absorption properties of the porphyrins, the complexes and the catenanes at 298 K in acetonitrile solution. The reported charge transfer (CT) bands arise from interaction of porphyrin with the paraquat or cyclobisparaquat unit.

	Soret bands	Q bands		CT bands
	λ_{max} [nm] (ε [$M^{-1}cm^{-1}$])	λ_{max} [nm] (ε [$M^{-1}cm^{-1}$])	λ_{max} [nm] (ε [$M^{-1}cm^{-1}$])	λ_{max} [nm] (ε [$M^{-1}cm^{-1}$])
MOD	412 (420000)	541 (18800)	577 (6200)	
4	414 (420000)	542 (17600)	577 (6000)	
5	413 (420000)	542 (19000)	577 (6000)	
6	413 (370000)	542 (17300)	577 (5700)	
4-PQ^{2+}	420 (224000)	546 (15000)	578 (5100)	720 (260)
5-PQ^{2+}	418 (257000)	544 (17000)	578 (6700)	720 (230)
6-PQ^{2+}	418 (234000)	543 (15000)	578 (5800)	720 (380)
Cat-**4**	425 (199700)	548 (21100)	582 (7400)	765 (600)
Cat-**5**	425 (209700)	548 (18800)	583 (5800)	760 (400)
Cat-**6**	425 (201000)	548 (21700)	582 (6900)	760 (500)

Table 2. Luminescence data in acetonitrile solutions (298 K) and butyronitrile solution (77 K) of porphyrins *n* and unstrapped model MOD.[10]

		298 K			77 K		
		λ_{max} [nm]	τ [ns]	Φ_{fluo}[a]	λ_{max} [nm]	τ [ns]	E [eV][b]
MOD	^{1}MOD	582	2.6	0.029	582	3.2	2.13
	^{3}MOD				728	46×10^6	1.70
4	^{1}**4**	584	2.1	0.030	582	2.4	2.13
	^{3}**4**				724	55×10^6	1.71
5	^{1}**5**	584	2.1	0.030	582	2.3	2.13
	^{3}**5**				728	70×10^6	1.70
6	^{1}**6**	584	2.0	0.030	582	2.2	2.13
	^{3}**6**				726	67×10^6	1.71

[a] Fluorescence quantum yield upon excitation at 413 and 542 nm, see Experimental Section for details. [b] Energy derived from the emission band maxima at 77 K.

+0.67 V versus SCE for **4**, **5**, and **6**, respectively. The first oxidation wave of the unstrapped porphyrin MOD, was detected at +0.60 V versus SCE; the lower value with respect to the strapped porphyrins could be assigned to the presence of the dimethoxyphenyl substituents on the *meso* positions, which makes the oxidation process easier. The values are in line with previously reported data of zinc *meso*-diaryloctaalkylporphyrin in butyronitrile.[9d]

No determination could be performed on the complexes since, in addition to the solubility problems, the modest association constant (10^2–10^4 M^{-1}) required too large a concentration of the excess reactant to provide a percentage of complexation (ca. 90–95%) such that the properties of the complexes could be determined with some reliability. In particular, to examine the reduction window (which, in DMF, could give more significant information) prohibitive amounts of the porphyrins are needed. In the discussion on electron transfer (see later) we will assume approximate values for the first oxidation of porphyrins in the complexes similar to the one determined here in DMF for the simple model porphyrins, that is +0.62, +0.65 and +0.67 V versus SCE for **4**-PQ^{2+}, **5**-PQ^{2+}, and **6**-PQ^{2+}, respectively. We are conscious that these are lower limits since the complexation by paraquat and the consequent CT interaction is expected to increase the oxidation potentials. Nonetheless CT interaction between the porphyrinic donor and the paraquat acceptor in the complexes, as testified by the modest stabilization of the CT bands detected at 720 nm (with respect to the stronger interaction detected for the catenanes where $\lambda_{max} = 760$ nm), is expected to be rather weak and negligible in the present context.

As far as the first reduction potential of PQ^{2+} is concerned, it is well documented that upon CT interaction with a dimethoxybenzene unit, the first reduction of paraquat type units is made more difficult by 0.1–0.08 V.[14] Accordingly, if we assume a value of −0.43 V for the first reduction of PQ^{2+} in acetonitrile,[12] its complexation in the strapped porphyrin unit should shift the first reduction to a more negative value of approximately −0.5 V.

Spectroscopic and photophysical characterization of Cat-*n*

Ground state absorption: The absorption data of the catenanes, Cat-*n*, are collected in Table 1 together with the data of the related porphyrin models *n*, and the complexes *n*-PQ^{2+}. Figure 2 displays the spectra of all catenanes described. To allow comparison with the models, for Cat-**6** only, the spectra of porphyrin **6**, and of the complex **6**-PQ^{2+} are shown. The

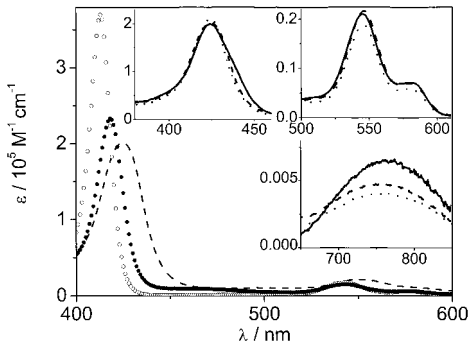

Figure 2. Absorption spectra of Cat-**6** (- - - -) compared with the absorption spectra of free **6** (○) and the complex **6**-PQ^{2+} (●). In the insets the spectra of the catenanes Cat-**4** (——), Cat-**5** (⋯⋯), and Cat-**6** (- - - -), are shown in the regions of the Soret bands, the Q bands and the CT bands.

catenane spectra display typical porphyrin Soret and Q bands. These appear broader, shifted to lower energies and with lower molar absorption coefficients than the model porphyrin *n* and, to some extent, also with respect to the complex *n*-PQ^{2+} (Table 1 and Figure 2). In the insets of Figure 2, the regions of the Q bands and the region at lower energy than the Q bands are enlarged, where new spectral features appear, for the three catenanes. These bands, which display maxima around 760 nm and molar absorption coefficients in the range 10^2–10^3 $M^{-1}cm^{-1}$, are assigned to CT bands that originate from the interaction between the porphyrin component and the para-

quat units of the macrocycle in the catenanes. Similar bands, though less intense and with maxima at higher energies, were also observed for the complexes (Table 1).[10] A stronger interaction is detected in the catenanes with respect to the complexes as revealed by the higher stabilization in the energy of the CT bands (i.e lower wavelength of the maximum), and the higher absorption coefficient. The reason for better stabilization in catenanes could be the higher oxidizing ability of $CBPQ^{4+}$ compared to that of PQ^{2+}, but to some extent geometric factors could also play a part. The rigidity of the catenane can ensure a better parallel orientation of the electron acceptor with the porphyrin plane, compared with the looser complex. Other CT bands, which are derived from the interaction between the $CBPQ^{4+}$ and the dimethoxy aromatic group in the 450–520 nm region, in agreement with previous observations,[12–13] are also detectable (Figure 2). The above features in the absorption spectra are indicative of interactions between the various components. Nonetheless, as confirmed below, the units maintain their own spectral and electrochemical features, indicating that the interaction between components, though active in promoting electronic coupling, can be considered a weak perturbation.

Luminescence: The porphyrin luminescence is quenched in the catenanes compared to that in the porphyrinic macrocycle alone, both at 298 and at 77 K, as shown for Cat-**5** in Figure 3. The steady-state residual luminescence at 298 K in acetonitrile is 1, 3, and 2% for Cat-**4**, Cat-**5**, Cat-**6**, respectively, compared to the model porphyrins **4**, **5**, and **6**. This reduction in the luminescence yield, Φ_{fluo}, could be consistent with a lifetime reduction of the porphyrin from approximately 2 ns (Table 2) to a few tens of picoseconds, according to the relation $\Phi_{fluo} = k_{rad}\tau$. Alternatively, an even larger decrease of

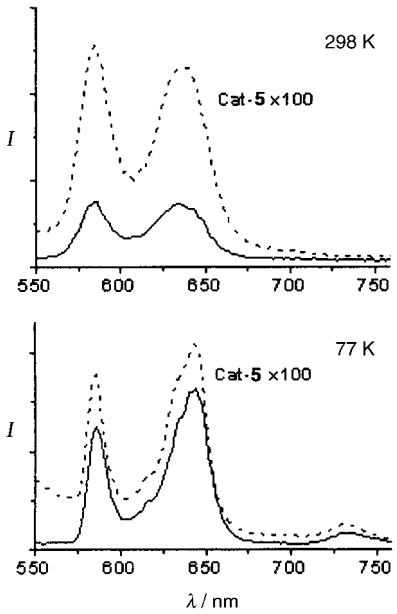

Figure 3. Luminescence quenching in the catenane Cat-**5** (----) at 298 and 77 K compared with the emission of an optically matched solution of **5** (——). The sensitivity is 100 times higher in the case of the catenane.

the lifetime in the catenanes but in the presence of a few percentage of free porphyrin macrocycle in the sample, could contribute to the steady-state emission.

An unambiguous answer can be obtained by time-resolved luminescence experiments with picosecond resolution. The time-resolved luminescence profiles in acetonitrile display a very fast decay in Cat-**5** and Cat-**6** which, after deconvolution with the instrumental profile, yields lifetimes of 20 ps. The luminescence decay and fit is shown for Cat-**6** in Figure 4. In

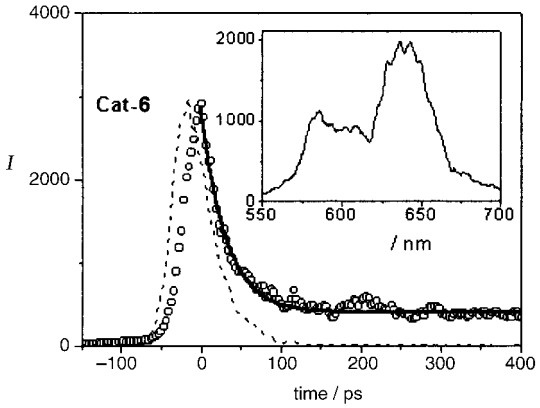

Figure 4. Luminescence decay at 650 nm of Cat-**6** (○) upon excitation with a 35 ps laser (532 nm, 1 mJ per pulse). The instrumental response (----) and the fitting (——) are shown. In the inset the spectrum in the time window 0–50 ps is reported.

Cat-**5** and Cat-**6** the fast decay is followed by a slower one, with a lifetime of approximately 2 ns, whose contribution is of the order of few percent[15] and can be ascribed to some contamination by the porphyrin component not engaged in the interlocked structure. In spite of the very short lifetime, just at the edge of our resolution of 20 ps, the determination corresponds to a genuine decay of a porphyrin type emission, as testified by the time-resolved spectrum at very short time periods. The time-resolved spectrum over the 0–50 ps time window, reported in the inset of Figure 4, indicates the presence of typical porphyrin emission bands. On the contrary, in the case of Cat-**4**, no such fast decay could be detected but only a very weak and long-lived (2 ns) luminescence was registered, ascribable to some residual free porphyrin macrocycle. This indicates that the quenching within the catenane Cat-**4**, measured by steady-state techniques to be 99%, occurs faster than our resolution (20 ps) within the laser pulse duration.

The quenching of the porphyrin luminescence in the catenanes is assigned to an electron-transfer reaction from the singlet excited state localized on the porphyrin, to the electron acceptor $CBPQ^{4+}$, hereafter called charge separation (CS). The reaction is faster than 20 ps in Cat-**4**, where the strap is shorter than in the other catenanes. Remarkably, the CS reaction is slower in the catenanes Cat-**5** and Cat-**6** than in the corresponding complexes, **5**-PQ^{2+} and **6**-PQ^{2+}, where we have been unable to time resolve the reaction as it is faster than our instrumental resolution and the decay occurs within the pulse.[10] The CS reaction lifetimes for the present catenanes and the previously studied complexes are summarized in Table 3.[10]

Table 3. Lifetimes of the charge separation (from time-resolved luminescence) and charge recombination (from transient absorbance) in the complexes *n*-PQ^{2+} and in the catenanes Cat-*n*.

	τ_{CS} [ps]	τ_{CR} [ps]
4-PQ^{2+}	< 20	< 20
5-PQ^{2+}	< 20	20
6-PQ^{2+}	< 20	20
Cat-**4**	< 20	39
Cat-**5**	20	37
Cat-**6**	20	45

Time-resolved absorption: The CS state formed by the electron-transfer reaction is characterized by a porphyrinic cation and a reduced paraquat-type radical. This is expected to display the characteristic absorption bands of the two radicals, respectively at 670 nm for the oxidized Zn^{II} porphyrin[16] and around 600 nm for the reduced paraquat radical.[17] The transient absorptions detected at the end of a 35 ps laser pulse, with excitation at 532 nm, are shown in Figure 5 for

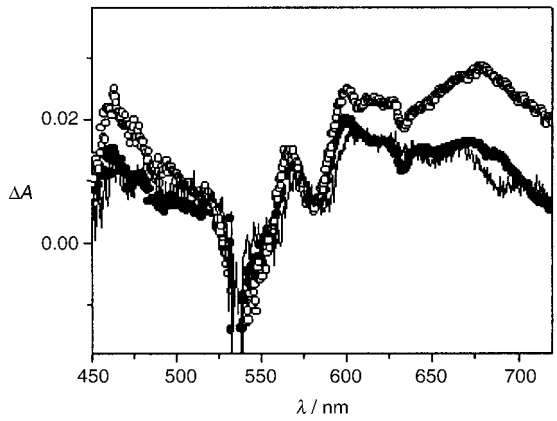

Figure 5. Transient absorbance of toluene solutions of Cat-**4** (——), Cat-**5** (○), Cat-**6** (●) upon excitation with a 35 ps pulse (532 nm, 3 mJ per pulse). The absorbance of the samples at the exciting wavelength was 0.8–0.9.

Cat-**4**, Cat-**5**, Cat-**6**. The signatures of the CS states with maxima at 600 and 670 nm can be detected and their time evolution can be registered. The decay of the transient absorbance features registered at 600 nm are reported in Figure 6 for the three catenanes. They can be fitted by exponential decays with lifetimes in the range of 37–45 ps which can be considered the same within experimental error.

The reaction is assigned to the recombination reaction of the charge-separated state, hereafter called CR, to yield once again the ground state. The base line is completely recovered and no residual signal from the triplet porphyrin or any other intermediate could be detected with a nanosecond flash-photolysis apparatus. The absence of any triplet porphyrin is in full agreement with the existence of the fast CS reaction which, by rapidly depleting the excited singlet state, does not allow any intersystem-crossing to the triplet state.

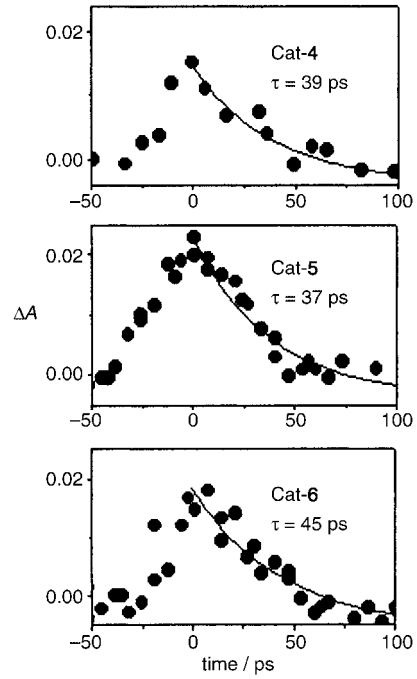

Figure 6. Decay of the charge separated state detected at 600 nm and exponential fittings for Cat-**4**, Cat-**5**, and Cat-**6**.

The lifetime of the CS state in the catenanes, 37–45 ps, although still very short, is longer than those of the corresponding complexes **4**-PQ^{2+}, **5**-PQ^{2+}, **6**-PQ^{2+}, which were measured to be < 20 ps for the complex with the shorter strap **4**-PQ^{2+} and only 20 ps for the other two complexes, see Table 3.

Electrochemical characterization of Cat-*n*

The catenanes Cat-**4**, Cat-**5**, and Cat-**6** exhibit very rich redox patterns, due to the presence of several different and interacting electro-active subunits (Figure 1, Table 4). In all the compounds, the bisbipyridinium macrocycle $CBPQ^{4+}$ plays the role of the electron acceptor subunit. Cat-**4** and Cat-**6** contain the same electron donor components, that is the substituted dimethoxynaphthalene (DMN) moiety, and the Zn porphyrin. Differences between Cat-**4** and Cat-**6** arise from the different dimensions of the macrocycles containing the electron donor groups (Figure 1). The electron-donor macrocycle that is present in Cat-**5** has the same dimensions as that which is present in Cat-**6**, with the noticeable difference that a substituted dimethoxybenzene (DMB) group replaces the DMN subunit. Clearly, the oxidation processes of the

Table 4. Electrochemical data.[a]

Compound	*E*(ox) (V versus SCE)	*E* (red) (V versus SCE)
$CBPQ^{4+}$		−0.28 [2]; −0.72 [2];
Cat-**4**	+0.72[1]; +1.06;[b] +1.67 [irr.]	−0.34[1]; −0.56[1]; −0.85 [2]; −1.70 [1];
Cat-**5**	+0.66[1]; +0.88;[b] +1.87 [irr.]	−0.32[1]; −0.39[1]; −0.82 [2];
Cat-**6**	+0.68[1]; +0.88;[b] +1.59 [irr.]	−0.35[1]; −0.45[1]; −0.76[1]; −0.86[1]; −1.68[1]

[a] $E_{1/2}$, values in acetonitrile. Potentials versus SCE. All the redox processes are reversible unless otherwise stated. The numbers in brackets refer to the number of exchange electrons. [b] Quasi-reversible processes.

catenanes involve the porphyrin and DMB (or DMN) subunits, whereas the reduction processes are localized on the bisbipyridinium subunits of the acceptor macrocycle.

Reduction processes: The electron acceptor macrocycle $CBPQ^{4+}$ contained in the catenanes investigated here is commonly used in catenane and rotaxane chemistry[18] and its properties are well known.[12–13, 19–21] For better comparison purposes, we re-examined the properties of the free electron acceptor macrocycle under our conditions (acetonitrile, room temperature) and found that it undergoes two bielectronic reversible processes at potentials (Table 4) close to those reported in the literature.[19, 20] The first process is the contemporary one-electron first reduction of each bipyridinium subunit and the second one is due to the contemporary one-electron second reduction of the same subunits.

In the free-electron acceptor macrocycle, the reduction processes have a bielectronic nature since the two bipyridinium units are equivalent to each other and are also weakly interacting. When such a macrocycle is a component of organized assemblies such as catenanes, the changes of its reduction "fingerprint" give useful information on the electronic interactions and the chemical environments that the electroactive subunits experience in the supramolecular arrays.

As pointed out by several groups,[11–14, 18–22], charge transfer (CT) interactions between the subunits play important roles in stabilizing the species in catenanes and rotaxanes containing donor and electron acceptor subunits. Such CT interactions are held responsible for the shift of the reduction potentials of Cat-**4**, Cat-**5**, and Cat-**6** with respect to the free bisbipyridinium macrocycle reductions (Table 4, Figures 7 and 8). The magnitude of this shift depends on the extent of the CT interactions.

The first bielectronic wave, typical of the free acceptor cyclophane, is also split in all the catenanes studied here into two monoelectronic processes (Table 4, Figures 7 and 8). This is because of the different (inside and outside) environments experienced by the bipyridinium subunits.[20] This also indicates that rotation of the acceptor cyclophane ring is inactive within the time scale of our measurements and confirms that in the stable conformation one bipyridinium unit is inside the porphyrin-containing macrocycle (*inner* subunit) and the other one is outside (*outer* subunit). It is reasonable to assume that the first reduction involves the outer bipyridinium subunit, while the second process involves the inner one, which is more difficult to reduce with respect to the former because it interacts with *two* electron donor groups (i.e., the porphyrin and the DMN, or DMB, subunits). The outer is involved in the CT interaction only with *one* electron donor group, that is the DMN (or DMB) subunit.

In the light of the above considerations, the slightly less negative potential (Δ20 mV, see Table 4) of the first reduction process of Cat-**5** compared to the corresponding process of Cat-**4** and Cat-**6** (for which the first reduction takes place at nearly the same potential) is attributed to the different electron donor properties of DMB and DMN; DMN is a better electron donor than the DMB unit. The same argument

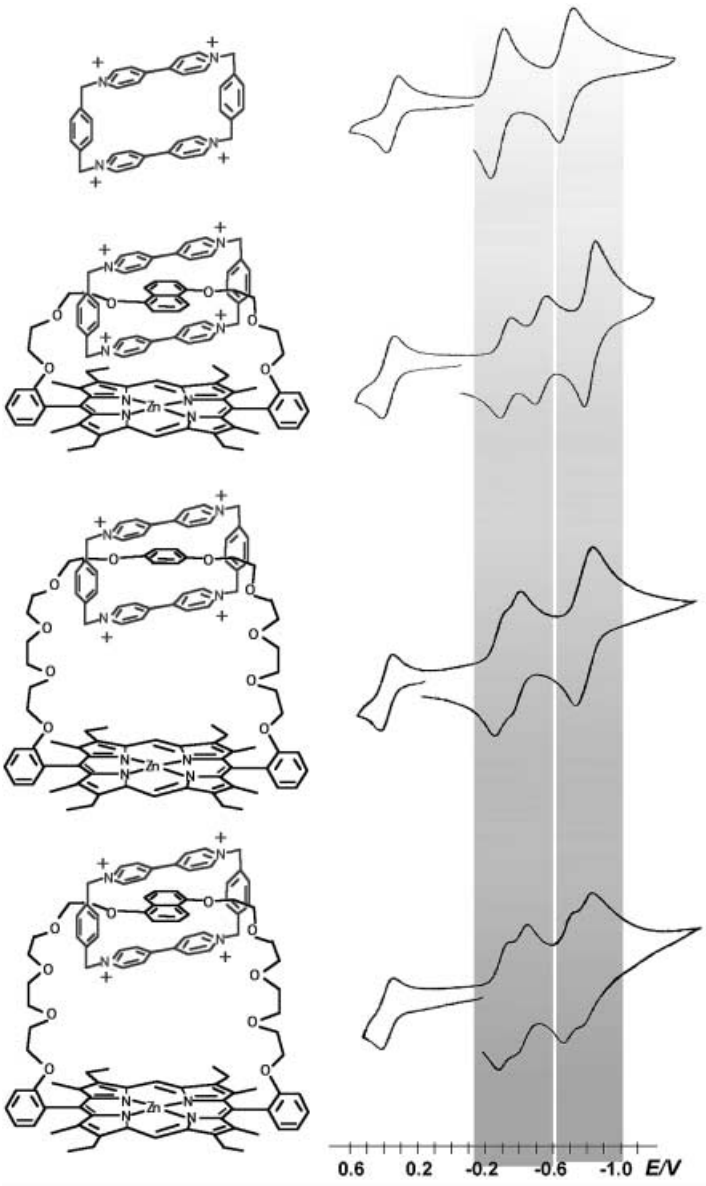

Figure 7. Cyclic voltammograms of the catenanes Cat-**4**, Cat-**5** and Cat-**6** in argon-purged acetonitrile solution. For comparison purposes, the cyclic voltammogram of the free electron acceptor macrocycle is also shown. Scan speed: 200 mV s^{-1}. The wave at +0.395 V is ferrocene, used as standard. Oxidation processes not shown.

accounts for the less negative potential of the second reduction process of Cat-**5** with respect to those of Cat-**4** and Cat-**6**. However, this second reduction process occurs at different potentials for Cat-**4** and Cat-**6** (Table 4). This can be justified by considering that in Cat-**4** the porphyrin donor is closer to the inner bipyridinium subunit (the redox site involved in the second reduction, see above) than in Cat-**6**. This is because of the constraints imposed by the different sizes of the macrocycles, and therefore the CT interaction between the porphyrin and bipyridinium subunits, which destabilizes the bipyridinium acceptor orbitals, is larger in Cat-**4**.

The third and fourth reductions of Cat-**6** are still reversible and monoelectronic, whereas the third reduction of Cat-**5** is also reversible, but bielectronic in nature (Table 4, Figures 7

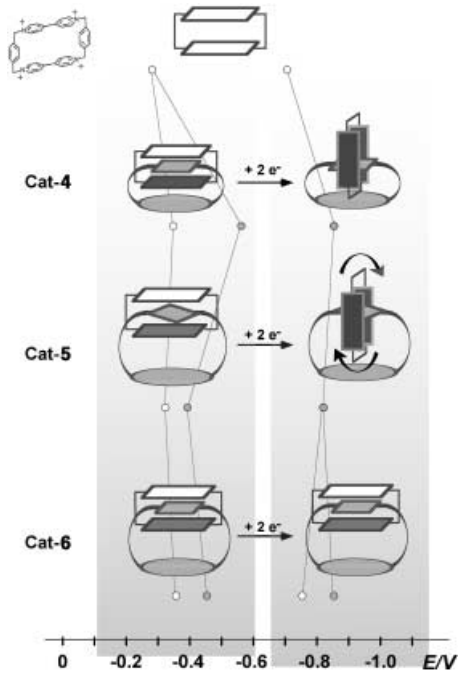

Figure 8. Genetic diagram of the reduction processes taking place in the catenanes studied here. Sketches of the proposed structures of the catenanes in the various states are superimposed. The oval represents the porphyrin ring; light grey rectangle is the DMN unit; distorted rectangle stands for the DMB unit; empty rectangles identify the bipyridinium subunits of the bis(bipyridinium) macrocycle. In the catenanes, the inner bipyridinium is represented as a grey rectangle and the outer one is still empty in order to stress the difference of their chemical environments. After the second reduction, Cat-**4** and Cat-**5** undergo structural reorganizations (see text). A possible new conformation for the doubly reduced Cat-**4** and Cat-**5** species is also shown. In these sketches the rectangles representing the bipyridinium subunits are both dark grey in order to stress their equivalence.

and 8). This suggests that, although the CT interactions are reduced in intensity following the first reduction of both the bipyridinium subunits of Cat-**6**, they are still strong enough to inhibit free rotation (or structural reorganization) of the interlocked rings within the time scale of our experiment. Therefore here, and also after the second reduction, inner and outer bipyridinium are still distinguishable in Cat-**6**, with the outer one responsible for the third reduction and the inner one responsible for the fourth process. Interestingly, the separation between the third and fourth reduction processes (100 mV) is comparable to the separation between the first and second processes (110 mV), indicating that the differences between inner and outer bipyridinium subunits remain constant upon first reduction. This is not the case for Cat-**5**. The bielectronic nature of its third reduction process indicates that the two bipyridinium subunits of Cat-**5** become equivalent after one-electron reduction of both such subunits. This can occur either by means of a relatively fast rotation of the cyclophane macrocycle or by a structural reorganization of the interlocked rings. The latter minimizes differences between the two bipyridinium subunits with respect to CT interactions, that is with respect to relative distances of the bipyridinium subunits from the porphyrin and DMB electron donors. Such a reorganization could be, for example, a 90° rotation of the cyclophane ring which could lead both the bipyridinium subunits to interact with both the porphyrin and DMB donors. (In a conformation which makes the two bipyridinium centers equivalent, it is not possible to distinguish between inner and outer bipyridinium subunits anymore, but both the acceptor components are partially inner and outer). Such a possible conformation is shown in Figure 8. The differences in the properties of Cat-**5** and Cat-**6** after the second reduction are still ascribed to the differences in donor capability of DMB and DMN. This behavior is in agreement with the findings reported for other catenanes containing similar subunits.[20]

The behavior of Cat-**4** after the second reduction is somewhat puzzling. The interaction between the cyclophane ring and the porphyrin and DMN units should be strong enough to inhibit the free rotation or structural reorganization of the array, as happens for Cat-**6** which contains the same redox-active subunits, the third reduction process is bielectronic. This indicates that in the case of Cat-**4**, similar to Cat-**5**, the first reduction of both bipyridinium subunits makes these subunits equivalent. The strong interaction between the donor porphyrin subunit and the cyclophane operating in Cat-**4** has to be responsible for this behavior. The extent of this interaction is also evident by comparing the potentials of the second reductions of Cat-**4** and Cat-**6**, see above. Probably the presence of the added electron on the inner bipyridinium subunit disturbs the interaction of such a unit with the porphyrin, so that a different conformation, in which the two bipyridinium subunits are equivalent, becomes preferred. The observation that in the new conformation the two acceptor sites are partially "inner" (see above) is supported by the coincidence of the potentials of the third reduction of Cat-**4** and of the fourth reduction of Cat-**6**.

An explanation of the differences observed for the third and fourth reductions within the series Cat-**4**, Cat-**5**, and Cat-**6** may lie in the data obtained from dynamic ^{1}H NMR measurements. We have measured rates of rotation at 25 °C for the three members of the series using the same procedures as previously reported,[11a] and they are $\ll 1$, 3×10^5, and 100 Hz, respectively. We have also demonstrated previously for an extended series of catenanes that while there is little difference between rotation rates for corresponding zinc and free base derivatives, protonation of the porphyrin units in the free-base derivatives has the effect of increasing the rotation rates. This is especially true for the DMB members of the series, but less so in the DMN series where they remain approximately unchanged.[11b] We rationalized this as an effect of protonation destroying any charge transfer interactions between the porphyrin and the tetrapositively charged $CBPQ^{4+}$ macrocycle and of introducing additional coulombic repulsions between the two components. In the DMN series, the stronger $\pi-\pi$ interactions are the limiting factor on rotation rates, which are little influenced by the porphyrin. Nevertheless, in Cat-**4**, the restrictions of the tight strap prevent any effective rotation at room temperature, in any of the free base, zinc, or protonated derivatives. It is not unreasonable to assume therefore that after the second reduction, rotation of the macrocycle in Cat-**4** is still severely restricted. On the other hand, we would predict, by analogy

with the protonation ^{1}H NMR experiments,[11b] that after the second reduction the rotation of the $CBPQ^{2+}$ macrocycle in Cat-**5** will be $\gg 10^5$ Hz. It would appear anomalous for both to experience a similar bielectronic third and fourth reduction, which implies equivalence of both bipyridinium subunits of the $CBPQ^{2+}$ macrocycle. The apparent paradox can be resolved however, by invoking a different mechanism by which equivalence is reached in each of two molecules. In Cat-**4**, a sideways orientation as depicted in Figure 8 would achieve such equivalence within an essentially "locked" (or very restricted) system. Rapid rotation in Cat-**5**, rather than locking in an end-on orientation, would achieve the required equivalence in this freely rotating system. As for Cat-**6**, it appears that although the charge transfer interactions between the $CBPQ^{2+}$ and both the porphyrin and the DMN group is weakened after the first and second reductions, there is sufficient flexibility and freedom in this system to allow the $CBPQ^{2+}$ macrocycle encircling the DMN unit to move away from the porphyrin, without resorting to an "end-on" orientation. This, together with the inherent restricted rotation about the DMN unit ($\approx$100 Hz for the Zn, free base and protonated free base derivatives measured in ^{1}H NMR studies), means that a more or less parallel orientation of all three units is maintained, giving rise to "inside" and "outside" environments for the bipyridinium subunits, and hence to two distinct monolectronic reductions.

In all the catenanes, at potentials more negative than -1.65 V versus SCE, a reversible monoelectronic reduction process, localized on the porphyrin subunit, occurs.

Oxidation processes: All the catenanes show three processes (Table 4). To assign the different oxidation processes to specific sites of the arrays it is useful to recall that the oxidations of DMN[21] and DMB[12] take place at $+1.17$ and $+1.31$ V versus SCE respectively. In the catenanes, the oxidation of the corresponding components (DMB and DMN) is expected to occur at even more positive potentials as a consequence of the CT interactions. The porphyrin units undergo the first oxidation process in DMF (see above) at $+0.62$, $+0.65$, and $+0.67$ V versus SCE for **4**, **5**, and **6**, respectively. Data in butyronitrile for a zinc *meso*-diaryloctaalkylporphyrin are available from the literature: $+0.63$ and $+1.02$ V versus SCE for the first and second oxidation wave respectively.[9d] Therefore, in all the cases investigated here, we can assign the first two oxidations to the porphyrin subunits and the third one to the DMN or DMB sites. In agreement with such an assignment it is useful to note that the first two processes occur at very similar potentials in Cat-**5** and Cat-**6** (the same redox-active site, that is the porphyrin subunit, is involved). Conversely, the potentials of the third process are quite different in the two species, with the one containing the better electron donor DMN center which is oxidized at less positive potential.

Interestingly, the porphyrin-centered oxidation processes in Cat-**4** take place at more positive potentials than in Cat-**5** and Cat-**6**. This demonstrates further that the extent of the CT interactions involving the porphyrin subunit in the former (smaller and more restricted) catenane is much stronger than in the other two.

Electron transfer in Cat-*n* and *n*-PQ^{2+}

On the basis of the luminescence properties at 77 K (Table 2) and of the electrochemical data discussed in the previous sections and reported in Table 4, schematic energy level diagrams for the two types of arrays, the noncovalently linked complexes *n*-PQ^{2+} and the mechanically bound Cat-*n*, can be drawn (Figure 9).

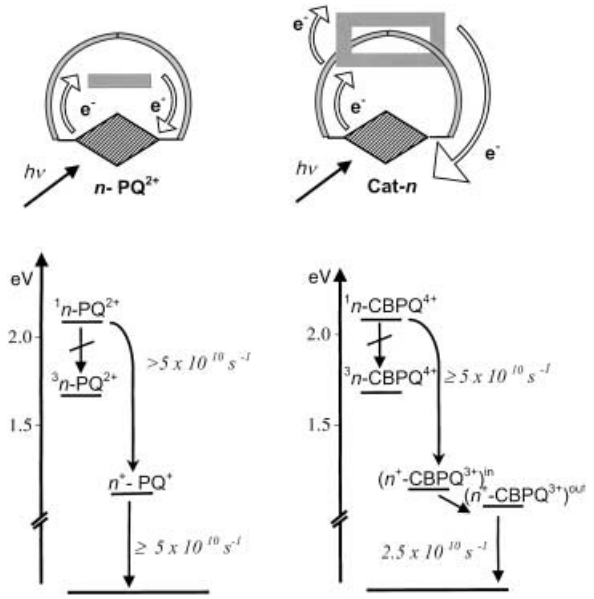

Figure 9. Schematic energy level diagrams and measured rate constants for the generic complex *n*-PQ^{2+} and the catenane Cat-*n*. The charge separated state $(n^{+}\text{-}CBPQ^{3+})^{in}$ corresponds to the reduction localized on the *internal* paraquat unit of the macrocycle, whereas $(n^{+}\text{-}CBPQ^{3+})^{out}$ corresponds to the reduction localized on the *external* paraquat unit of the macrocycle.

The excited energy levels are essentially identical in the two diagrams, respectively 2.13 eV for the singlet localized on the porphyrin unit, and 1.7 eV for the related triplet excited state. The excited states of the electron acceptor unit are not relevant to the present case since the excitation occurs in the visible region of the spectra, where only porphyrin components absorb light.

The energy level of the CS state can be calculated by simply adding the energy necessary to oxidize the electron donor, to the energy necessary to reduce the electron acceptor.[23, 24] As far as the estimate of the CS state for *n*-PQ^{2+} is concerned, only approximate figures can be derived given the lack of electrochemical data for the complexes (see Model Section). Nonetheless the potentials of the oxidation processes of the porphyrin models in DMF are available ($+0.62$ V versus SCE for **4**, $+0.65$ V versus SCE for **5**, and $+0.67$ V versus SCE for **6**) and a reduction potential for paraquat in the complex of the order of -0.5 V versus SCE can be assumed (see Model Section). The use of potentials determined for porphyrin hosts does not take into consideration the destabilizing effect due to CT interactions in the complexes, expected to be higher for the short strap component **4**-PQ^{2+}. Since strapped porphyrin **4** undergoes oxidation at a less positive potential than **5** and **6**, this in part is expected to counterbalance the destabilizing

larger effect of CT interactions. On this basis and in the frame of a qualitative approach, the energy for the charge separated sates n^+-PQ^+ can be assumed similar for all the complexes and of the order of approximately 1.15 eV.[23, 24]

For the catenanes Cat-*n*, it is evident from the data reported in Table 4 that two very close charge-separated states exist, the first at lower energies corresponding to the oxidized porphyrin and the reduced *outer* paraquat unit of the cyclobisparaquat, $(n^+\text{-}CBPQ^{3+})^{out}$, and the second corresponding to the oxidized porphyrin and the *inner* paraquat unit of the macrocycle, $(n^+\text{-}CBPQ^{3+})^{in}$. The latter CS has energy values of 1.28 eV for Cat-**4**, 1.05 eV for Cat-**5**, and 1.13 eV for Cat-**6**, while the energy levels of the former are stabilized, respectively at 1.06 eV for Cat-**4**, 0.98 eV for Cat-**5**, and 1.03 eV for Cat-**6**.

Therefore the two energetic diagrams of Figure 9 are similar, but in the case of the catenane the low-lying charge-separated state is split because of the nonequivalence of the reduction sites in the cyclic electron acceptor. The less stabilized CS involves reduction of the paraquat unit interposed between the porphyrin and the DMN (or DMB) planes which, because of the closer approach to the porphyrin electron donor, is expected to be involved in the primary transfer of electron from the porphyrin excited state, the CS reaction. The splitting between the CS states is different for the various catenanes. This is important in Cat-**4**, with a value of 0.22 eV, due to the stronger interaction caused by a closer approach of partners constrained by the shorter strap, whereas it has smaller values in Cat-**6** (0.1 eV) and Cat-**5** (0.07 eV).

Comparison of the energy levels and related thermodynamic parameters in *n*-PQ^{2+} and Cat-*n* indicates that charge-separated states in the complexes are, roughly, at a higher energy than both levels of the catenanes for the longer strapped porphyrins **5** and **6**, and at an energy which is intermediate between the two levels for short-strapped **4**. The more facile reduction of the electron acceptor $CBPQ^{4+}$ with respect to PQ^{2+} is in part counterbalanced by the stronger CT interaction in the interlocked compounds, which is rather strong in Cat-**4**. The ΔG^0 value for CS is approximately -1.1 eV for *n*-PQ^{2+} and assuming a primary electron transfer from the porphyrin excited state to the adjacent (*inner*) paraquat unit of $CBPQ^{4+}$, the ΔG^0 value for CS ranges from -0.85 eV in Cat-**4**, to -1.08 eV in Cat-**5**, and -1 eV for Cat-**6**.

Regarding the CR reaction, the ΔG^0 is approximatley -1.5 eV for *n*-PQ^{2+} and, if we assume that in the catenanes the charge recombination reaction occurs from the more stabilized CS state, values of ΔG^0 of -1.06 eV in Cat-**4**, -0.98 eV in Cat-**5**, and -1.03 eV in Cat-**6**, can be derived. The above assumptions would obviously imply that within the catenanes, an electron transfer from the *inner* to the *outer* paraquat unit occurs fast, following the primary photoinduced transfer and we will discuss this point below.

The ΔG^0 value for CS and CR reactions are very high for both interlocked and complexed structures and both can be safely assumed to occur in a nearly activationless regime.[25] Therefore they will occur at the maximum rate regardless of the small differences in ΔG^0 attributable to the specific reaction. On such grounds the differences in the kinetic parameters determined for the single systems can be discussed solely based on the different structures of the assemblies.

The electron transfer rates determined for CS and CR are reported in Figure 9. In the complexes *n*-PQ^{2+} the CS rate is in all cases $> 5 \times 10^{10}\ s^{-1}$, as can be derived from the fact that no accumulation of luminescent species is detected during the short laser pulse (resolution 20 ps). A similar lower limit for the rate can be derived for the Cat-**4** interlocked structure, while in the other catenanes Cat-**5** and Cat-**6**, a rate of $5 \times 10^{10}\ s^{-1}$ can be measured from a lifetime of 20 ps. For CR a rate of recombination to the ground state of $5 \times 10^{10}\ s^{-1}$ could be measured for the complexes with the longer straps **5**-PQ^{2+},and **6**-PQ^{2+}, whereas **4**-PQ^{2+} recombined faster than the apparatus resolution, placing a lower limit of $5 \times 10^{10}\ s^{-1}$ to the rate.[10] The recombination in the catenanes is slower and detectable in all cases, Figure 6, and the same rate of $2.5 \times 10^{10}\ s^{-1}$ for Cat-**4**, Cat-**5** and Cat-**6** is measured.

In general terms, the complexes display a more rapid electron transfer than the catenanes both in CS and in CR reactions, and within the *n*-PQ^{2+} series the compound with a shorter strap displays a faster reaction. In the case of the catenanes this is also true for the charge separation reaction but not for charge recombination, where a similar rate is measured for all the systems, irrespective of the strap length.

In the complexes, where the association occurs by multiple weak interactions (primarily $\pi-\pi$, $C-H\cdots O$ hydrogen bonds, and electrostatic interactions) the electron acceptor experiences a "loose" situation that allows a closer approach to the porphyrin. This is a better electron donor than the dioxyaromatic unit contained in the strap (see Electrochemistry Section), favoring the rapid transfer of the electron to form the charge separated state. Only in the case of the "looser" strapped **5**-PQ^{2+}, and **6**-PQ^{2+}, the reduced paraquat radical, positively charged, which experiences some repulsion from the positively charged oxidized porphyrin has enough spatial freedom to be able to distance itself from its partner and can thus survive long enough to be detected by our apparatus. In the complex with the shorter strap this is not possible and both forward, CS, and back, CR, electron transfer reactions are extremely fast.

On the other hand, in the Cat-***n*** case, the mechanical linkage enforces the macrocyclic electron acceptor unit close to the dioxyaromatic residue and keeps it spatially separated from porphyrin donor. This allows a detectable CS reaction, except in Cat-**4** where the *inner* paraquat unit accepting the electron is very close to the porphyrin plane, because of the short strap. Once the electron has been transferred from the porphyrin donor to the *inner* paraquat unit of the macrocycle a *further* electron transfer step to the *outer* paraquat unit has to be postulated. This is necessary to explain the lifetime of the CR reactions which is essentially identical for all the catenanes, irrespective of the strap length (Figure 9). We do not expect to have spectroscopic evidence for this electron transfer since both inner and outer reduced paraquat units should display essentially identical absorption spectra. The proof is therefore indirect, but supported by the comparison with the corresponding complexes *n*-PQ^{2+}. If this further, postulated electron transfer were not to occur, the reactivity order detected for the complexes would still hold, with Cat-**4**

reacting much faster than Cat-**5** and Cat-**6**, due to the close proximity of the inner paraquat to the porphyrin.

This postulated electron transfer step further separates the charges in space and allows a slower recombination in all the catenanes. In this regard it should be pointed out that the time scale of electron transfer is much faster than any structural reorganization discussed in the Electrochemistry Section.

Conclusion

A series of catenanes containing a macrocyclic porphyrin and the electron acceptor cyclo*bis*(paraquat-*p*-phenylene) has been spectroscopically, photophysically and electrochemically characterized. The electron transfer rates leading to charge separation and the recombination rate to the ground state have been determined.

Comparison with closely related complexes containing the same porphyrin macrocycles and paraquat as electron acceptor is made. Assuming that thermodynamic parameters are not effective in determining the different observed rates (activationless region), the results are discussed on the basis of structural differences of the interlocked and complexed structures, respectively. The rates of electron transfer are faster in the complexes than in the catenanes and this is attributed to a looser structure in the complexes which favors a closer approach of the partners in the charge-separation reaction. Accordingly, a slower charge-separation reaction is measured in the systems with longer straps and the same occurs for the recombination reaction of the charge-separated state in the complexes. This recombination reaction in the catenanes occurs with the same rate regardless of the strap length and suggests the involvement of a further, subsequent electron transfer to a more stabilized reduction site of the macrocyclic electron acceptor, identified as the outer paraquat unit of the cyclic electron acceptor $CBPQ^{4+}$.

Experimental Section

The synthesis and characterization of these and closely related porphyrins, complexes and catenanes have been reported and discussed previously.[11, 26]

Spectroscopic and photophysical determinations: Acetonitrile Spectroscopic Grade (C. Erba) was used. Absorption spectra were recorded with a Perkin-Elmer Lambda 9 spectrophotometer and emission spectra, uncorrected if not otherwise specified, were detected by a Spex Fluorolog II spectrofluorimeter equipped with a Hamamatsu R 928 photomultiplier. Relative luminescence intensities were evaluated from the area (on an energy scale) of the luminescence spectra corrected for the photomultiplier response. Luminescence quantum yields ϕ for the components were obtained with reference to a standard, Zn^{II} (1,5,10,15-tetra-*tert*-butylphenyl)porphyrin, in toluene with $\phi = 0.08$.[8f]

Fluorescence lifetimes longer than 1 ns were detected by an IBH Time Correlated Single Photon Counting apparatus with excitation at 337 nm. Luminescence lifetimes shorter than one nanosecond were determined by an apparatus based on a Nd:YAG laser (Continuum PY62 – 10) with a 35 ps pulse duration, 532 nm, 1 mJ per pulse and a Streak Camera. In a typical experiment, the luminescence signals from 1000 laser shots were averaged and the time profile was measured from the streak image in a wavelength range of approximately 20 nm around the selected wavelength. Spectra in a selected time window were also acquired from the streak image, which were based on a rectangular matrix of 480 points (wavelength) time 512 points (time). The fitting of the luminescence decays were performed by standard iterative non-linear programs taking into consideration the instrumental response. Further details on the equipment can be found elsewhere.[27]

Transient absorbance in the picosecond range made use of a pump and probe system based on a Nd-YAG laser (35 ps pulse, 532 nm, 2 – 4 mJ) and an OMA detector. The instrumental response profile was obtained by measuring the buildup of the absorption of the reference porphyrin (*n*) singlet at 600 nm and time zero was set at the complete evolution of the absorbance signal. Further details can be found elsewhere.[28] Estimated errors are 10 % on lifetimes and 20 % on quantum yields.

Electrochemical determinations: Electrochemical measurements on the catenanes were carried out in argon-purged acetonitrile at room temperature with a PAR 273 multipurpose equipment interfaced to a PC. The working electrode was a glassy carbon (8 mm^2, Amel) electrode. The counter electrode was a Pt wire, and the reference electrode was an SCE separated with a fine glass frit. The concentration of the samples was about 5×10^{-4} M. Tetrabutylammonium hexafluorophosphate was used as supporting electrolyte and its concentration was 0.05 M. Cyclic voltammograms were obtained at scan rates of 20, 50, 200, and 500 $mV\,s^{-1}$. For reversible processes, half-wave potentials (versus SCE) were calculated as the average of the cathodic and anodic peaks. The criteria for reversibility were the separation of 60 mV between cathodic and anodic peaks, the close to unity ratio of the intensities of the cathodic and anodic currents, and the constancy of the peak potential on changing scan rate. The number of exchanged electrons was measured with differential pulse voltammetry (DPV) experiments performed with a scan rate of 20 $mV\,s^{-1}$, a pulse height of 75 mV, and a duration of 40 ms, and by taking advantage of the presence of ferrocene used as the internal reference.

The determination of electrochemical properties of the model porphyrins could be only performed in dimethylformamide (DMF) for solubility reasons.

Acknowledgement

This work was financed by Italian CNR, the Australian Research Council and EC-TMR Research Network Program (contract No. ERB-FMRX-CT98-0226). The contribution of grant Agenzia2000 CNRC00B91D 004 to L.F is gratefully acknowledged.

[1] a) V. Balzani, F. Scandola, *Supramolecular Photochemistry*, Ellis Horwood, Chichester, **1991**; b) M. R. Wasielewski, *Chem. Rev.* **1992**, *92*, 435 – 461; c) D. Gust, T. A. Moore, A. L. Moore, *Acc. Chem. Res.* **1993**, *26*, 198 – 205; d) H. Kurreck, M. Huber, *Angew. Chem*. **1995**, *107,* 992 – 946; *Angew. Chem. Int. Ed. Engl.* **1995**, *34*, 849 – 866; e) A. Harriman, J.-P. Sauvage, *Chem. Soc. Rev.* **1996**, 41 – 48.

[2] a) J. Deisenhofer, H. Michel, *Angew. Chem.* **1989**, *101*, 872 – 890; *Angew. Chem. Int. Ed. Engl*. **1989**, *28*, 829 – 847; b) R. Huber, *Angew. Chem*. **1989**, *101*, 849 – 870; *Angew. Chem. Int. Ed. Engl*. **1989**, *28*, 848 – 869.

[3] a) W. Kühlbrandt, D. N. Wang, Y. Fujiyoshi, *Nature* **1994**, *367*, 614 – 621; b) G. McDermott, S. M. Prince, A. A. Freer, A. M. Hawthornthwaite-Lawless, M. Z. Papiz, R. J. Cogdell, N. W. Isaacs, *Nature* **1995**, *374*, 517 – 521; c) T. Pullerits, V. Sundström, *Acc. Chem. Res.* **1996**, *29*, 381 – 389.

[4] J. Weiss, *J. Inclusion Phenom. Macrocyclic Chem.* **2001**, *40*, 1 – 22.

[5] a) H. L. Anderson, *Chemm. Commun.* **1999**, 2323 – 2330; b) A. Tsuda, A. Osuka, *Science* **2001**, *293*, 79 – 82.

[6] a) K. Kalyanasundaram, *Photochemistry of Polypyridine and Porphyrin Complexes,* Academic Press, London, **1992**, pp 369 – 603; b) *The Porphyrin Handbook* (Eds.: K. M. Kadish, K. M. Smith, R. Guillard), Academic Press, San Diego, **2000**.

[7] a) C. J. Chang, J. D. K. Brown, M. C. Y. Chang, E. A. Baker, D. G. Nocera in *Electron Transfer in Chemistry* Volume III, part 2 (Ed.: V. Balzani), Wiley-VCH, Weinheim, **2001**, pp 409 – 46; b) M. D. Ward, *Chem. Soc. Rev.* **1997**, *26*, 365 – 375, and references therein; c) T. Hayashi, H. Ogoshi, *Chem. Soc. Rev.* **1997**, *26*, 365 – 375, and

references therein; d) R. A. Haycock, A. Yartsev, U. Michelsen, V. Sundström, C. A. Hunter, *Angew. Chem.* **2000**, *112*, 3762–3765; *Angew. Chem. Int. Ed. Engl.* **2000**, *39*, 3616–3619; e) C. A. Hunter, R. K. Hyde, *Angew. Chem.* **1996**, *108*, 2064–2067; *Angew. Chem. Int. Ed. Engl*. **1996**, 35, 1936–1939; f) F. Felluga, P. Tecilla, L. Hillier, C. A. Hunter, G. Licini, P. Scrimin, *Chem. Commun*. **2000**, 1087–1088; g) Y. Kuroda, K. Sugon, K. Sasaki, *J. Am. Chem. Soc.* **2000**, *122*, 7833–7834; h) A. Prodi, M. T. Indelli, C. J. Kleverlaan, F. Scandola, E. Alessio, T. Gianferrara, L. G. Marzilli, *Chem. Eur. J.* **1999**, *5*, 2668–2679; i) L. Flamigni, M. R. Johnston, L. Giribabu, *Chem. Eur. J.* **2002**, *8*, 3938–3947; j) L. Flamigni, A. M. Talarico, F. Barigelletti, M. R. Johnston, *Photochem. Photobiol. Sciences* **2002**, *1*, 190–197.

[8] a) G. Kodis, P. L. Lidell, L. de la Garza, P. C. Clausen, J. S. Lindsey, A. L. Moore, T. A. Moore, D. Gust, *J. Phys. Chem*. **2002**, *106*, 2036–2048; b) H. Imamori, D. M. Guldi, K. Tamaki, Y. Yoshida, C. Luo, Y. Sakata, S. Fukuzumi, *J. Am. Chem. Soc*. **2001**, *123*, 6617–6628; c) A. Nakano, A. Osuka, T. Yamazaki, Y. Nishimura, S. Akimoto, I. Yamazaki, A. Itaya, M. Murakami, H. Miyasaka, *Chem. Eur. J.* **2001**, *7*, 3134–3151; d) K. Kilså, J. Kajanus, A. Macpherson, J. Mårtensson, B. Albinsson, *J. Am. Chem. Soc*. **2001**, *123*, 3069–3080; e) D. Holten, D. F. Bocian, J. S. Lindsey, *Acc. Chem. Res.* **2002**, *35*, 57–69; f) I. M. Dixon, J.-P. Collin, J-P. Sauvage, L. Flamigni, *Inorg. Chem*. **2001**, *40*, 5507–5517; g) M.-S. Choi, T. Aida, T. Yamazaki, I. Yamazaki, *Chem. Eur. J*. **2002**, *8*, 2668–2678; h) L. Flamigni, G. Marconi, I. M. Dixon, J.-P. Collin, J.-P. Sauvage, *J. Chem. Phys. B* **2002**, *106*, 6663–6671.

[9] a) J.-C. Chambron, A. Harriman, V. Heitz, J.-P. Sauvage, *J. Am. Chem. Soc.* **1993**, 115, 6109–6114; b) E. Kaganer, E. Joselevich, I. Willner, Z. Chen, M. J. Gunter, T. P. Jeynes, M. R. Johnston, *J. Phys. Chem. B* **1998**, *102,* 1159–1165; c) G. Hungerford, M. Van der Auweraer, D. B. Amabilino, *J. Porphyrins Phtalocyanins* **2001**, *5*, 633–644; d) L. Flamigni, N. Armaroli, F. Barigelletti, J.-C. Chambron, J.-P. Sauvage, N. Solladie, *New J. Chem.* **1999**, *23,* 1151–1158; e) M. Linke, M., J.-C. Chambron, V. Heitz, J.-P Sauvage, S. Encinas, F. Barigelletti, L. Flamigni, *J. Am. Chem. Soc.* **2000**, *122*, 11834—11844; f) M. Andersson, M. Linke, J.-C. Chambron, J. Davidsson, V. Heitz, L. Hammarström, J.-P. Sauvage, *J. Am. Chem. Soc.* **2002**, *124*, 4347–4362.

[10] L. Flamigni, A. M. Talarico, M. J. Gunter, M. R. Johnston, T. P. Jeynes, *New J. Chem.* **2003**, *27*, 551–559.

[11] a) M. J. Gunter, D. C. R. Hockless, M. R. Johnston, B. W. Skelton, A. H. White, *J. Am. Chem. Soc.* **1994**, *116*, 4810–4823; b) M. J. Gunter, M. R. Johnston. *Chem. Commun.* **1994**, 829–830.

[12] P. L. Anelli, P. R. Ashton, R. Ballardini, V. Balzani, M. Delgado, M. T. Gandolfi, T. T. Goodnow, A. E. Kaiser, D. Philp, M. Pietraszkiewicz, L. Prodi, M. V. Reddington, A. M. Z. Slawin, N. Spencer, J. F. Stoddart, C. Vicent, D. J. Williams, *J. Am. Chem. Soc*. **1992**, *114*, 193–218.

[13] See for example: a) R. Ballardini, V. Balzani, M. T. Gandolfi, L. Prodi, M. Venturi, D. Philp, H. Rickett, J. F. Stoddart *Angew. Chem.* **1993**, *105*, 1362–1364; *Angew. Chem. Int. Ed. Eng.* **1993**, *32*, 1301–1303; b) Y-Z. Hu, S. H. Bossman, D. van Loyen, O. Schwarz, H. Durr, *Chem. Eur. J.* **1999**, *5*, 1267–1277.

[14] a) P. R. Ashton, R. Ballardini, V. Balzani, M. Belohradský, M. T. Gandolfi, D. Philp, L. Prodi, F. M. Raymo, M. Reddington, N. Spencer, J. F. Stoddart , M. Venturi, D. J. Williams, *J. Am. Chem. Soc.* **1996**, *118*, 4931–4951; b) P. R. Ashton, R. Ballardini, V. Balzani, A. Credi, K. R. Dress, E. Ishov, C. J. Kleverlaan, O. Kocian, J. A. Preece, N. Spencer, J. F. Stoddart , M. Venturi, S. Wenger, *Chem. Eur. J.* **2000**, *6,* 3558–3570.

[15] The apparent higher contribution of the long lifetime of 2 ns to the overall decay is due to the partial decay during the pulse of the short lifetime component of 20 ps.

[16] See, for example, ref. [1b], [8f], [9e].

[17] a) J. A. Farrington, M. Ebert, E. J. Land, *J. Chem. Soc. Faraday Trans. I* **1978**, *74*, 665–675; b) M. Venturi, Q. G. Mulazzani, M. Z. Hoffman, *Rad. Phys. Chem*. **1984**, *23*, 229–236.

[18] *Struct. Bonding* (*Berlin*) **2001**, *99*, 1–281 (special issue).

[19] a) V. Balzani, A. Credi, F. M. Raymo, J. F. Stoddart, *Angew. Chem.* **2000**, *112*, 3484–3530; *Angew. Chem. Int. Ed. Engl.* **2000**, *39*, 3348–3391, and references therein; b) R. Ballardini, V. Balzani, A. Credi, M. T. Gandolfi, M. Venturi, *Acc. Chem. Res.* **2001**, *34*, 445–455.

[20] P. R. Ashton, R. Ballardini, V. Balzani, A. Credi, M. T. Gandolfi, S. Menzer, L. Pérez-Garcia, L. Prodi, J. F. Stoddart, M. Venturi, A. J. P. White, D. J. Williams, *J. Am. Chem. Soc.* **1995**, *117*, 11171–11197.

[21] P. R. Ashton, M. Blower, D. Philp, N. Spencer, J. F. Stoddart, M. S. Tolley, R. Ballardini, M. Ciano, V. Balzani, M. T. Gandolfi, L. Prodi, C. H. McLean, *New J. Chem.* **1993**, *17*, 689–695.

[22] I. Willner, E. Kaganer, E. Joselevich, H. Dürr, E. David, M. J. Günter, M. R. Johnston, *Coord. Chem. Rev.* **1998**, *171*, 261.

[23] Taking into consideration the correction for Coulombic stabilization and change in solvent dielectric constant according to Weller, see ref [24], a correction of the order of tens of mV should be applied to the CS energy level, well below the approximation involved in the present case.

[24] A. Weller, *Z. Phys. Chem. NF* **1982**, *133*, 93–98.

[25] The term "activationless" is used in current theoretical models of electron transfer reactions, see for example: R. A Marcus, N. Sutin, *Biochim. Biophys. Acta* **1985**, *811*, 265–322 and references therein.

[26] a) M. J. Gunter, T. P. Jeynes, M. R. Johnston, P. Turner, Z. Chen, *J. Chem. Soc. Perkin Trans. 1,* **1998**, 1945–1957; b) M. J. Gunter, M. R. Johnston, B. W. Skelton, A. H. White, *J. Chem. Soc. Perkin Trans. 1* **1994**, 1009–1018; c) M. J. Gunter; M. R. Johnston, *J. Chem. Soc. Perkin Trans. 1* **1994**, 995–1008.

[27] L. Flamigni, *J. Phys. Chem*. **1993**, *97,* 9566–9572.

[28] L. Flamigni, N. Armaroli, F. Barigelletti, V. Balzani, J.-P. Collin, J.-O. Dalbavie, V. Heitz, J.-P. Sauvage *J. Phys. Chem. B.* **1997**, *101*, 5936–5943.

Received: October 16, 2002
Revised: January 17, 2003 [F4502]

